

***In situ* analysis with portable Raman and ED-XRF spectrometers for the diagnosis of the formation of efflorescence on walls and wall paintings of the Insula IX 3 (Pompeii, Italy)[†]**

Juan Manuel Madariaga,^{a*} Maite Maguregui,^b Silvia Fdez-Ortiz de Vallejuelo,^a Ulla Knuutinen,^c Kepa Castro,^a Irantzu Martinez-Arkarazo,^a Anastasia Giakoumaki^a and Africa Pitarch^a



This work presents the results of field Raman analyses, assisted by a hand-held energy dispersive X-ray fluorescence spectrometer, for the experimental determination of efflorescence from walls and wall paintings of two Pompeian houses, one with many luxurious decorative elements (House of Marcus Lucretius, Regio IX, Insula 3, House 5/24) and a more modest building (Regio IX, Insula 3, House 1-2). Both exposed and protected rooms were measured in different year seasons, spring (May 2010) and summer (September 2011 and 2012) and considering different orientations. Chemical attacks of acid gases (CO₂, SO₂ and NO_x) on the original compounds of the mortars, biominerals formed by the biological colonizations as well as direct rain-wash of the newly formed salts can be considered the three most serious problems of the archaeological remains from Insula IX 3 of Pompeii. Also, infiltration waters from the ground contribute to such decay. The walls and wall paintings exposed to the rain-wash are the worst preserved, probably as a result of a continuous cycle of CO₂, SO₂ and NO_x acid attack to the original carbonate materials, involving loss of plaster. This severe decay was not observed in the rooms covered by roofs although those walls affected by infiltration waters from the ground showed decaying because of the action of the efflorescence on the carbonate materials acting as the binder of the mural painting remains in the houses of Pompeii. Copyright © 2014 John Wiley & Sons, Ltd.

Additional supporting information may be found in the online version of this article at the publisher's web site.

Keywords: field analysis; portable Raman spectroscopy; wall paintings; efflorescence; environmental impacts

Introduction

The pyroclastic deposits of Mount Vesuvius buried the ancient city of Pompeii (Italy) during the eruption of 79 AD. Those deposits have preserved wall paintings and houses until their excavation.^[1] From the moment that an archaeological site is brought to light, it suffers deterioration as a result in part of rainfall, humidity, water infiltrations, etc., but mainly because of environmental stressors. Modern polluted atmospheres can also affect the conservation state of artworks and historical buildings. This has been the case of Pompeii where the beautiful walls and wall paintings have been exposed to open air from the time they were excavated and subsequently have been affected by the high polluted atmosphere of Naples and surroundings.

The recent literature reports the chemical transformations suffered by some pigments, describing the darkening of the two Pompeian red pigments, cinnabar (HgS) and iron red oxide (red ochre, hematite, α -Fe₂O₃). The blackening of cinnabar is attributed to the *in situ* formation of Hg⁰ by a chemical reduction process where terlinguaite (Hg₂ClO), corderoite (Hg₃S₂Cl₂) and calomel (Hg₂Cl₂) compounds are formed as side reaction products; these compounds have been detected in several wall paintings containing red cinnabar, and their formation by physico-chemical reactivity has been proposed elsewhere.^[2–4] The blackening of hematite is because of the *in situ* chemical reduction to magnetite (Fe₃O₄) by the atmospheric SO₂ acid

gas, as a recent work has demonstrated.^[5] Moreover, hematite can also be transformed into (para)coquimbite (Fe₂(SO₄)₃·9H₂O) if gypsum (CaSO₄·2H₂O) is present.^[4,5] All these chemical transformations have been experimentally demonstrated by accelerated ageing experiments of recently excavated (2007) wall painting fragments that have not been in contact with modern polluted atmospheres; the mentioned laboratory experiments were conducted as a function of relative humidity and SO₂ concentrations.^[6]

* Correspondence to: Juan Manuel Madariaga, Department of Analytical Chemistry, Faculty of Science and Technology, University of the Basque Country UPV/EHU, P.O. Box 644, 48080 Bilbao, Basque Country, Spain
E-mail: juanmanuel.madariaga@ehu.es

[†] This article is part of the special issue of the Journal of Raman Spectroscopy entitled "Raman in Art and Archaeology 2013" edited by Polonca Ropret and Juan Manuel Madariaga.

a Department of Analytical Chemistry, Faculty of Science and Technology, University of the Basque Country UPV/EHU, P.O. Box 644, 48080, Bilbao, Basque Country, Spain

b Department of Analytical Chemistry, Faculty of Pharmacy, University of the Basque Country UPV/EHU, P.O. Box 450, 01080, Vitoria-Gasteiz, Basque Country, Spain

c Department of Art and Cultural Studies, University of Jyväskylä, PL 25, Jyväskylä 40014, Finland

Other studies on roman wall paintings of the Vesuvian area report the identification of mineralogical compounds that cannot be considered original in most of the plasters.^[7–9] Such compounds were also identified by the authors at a laboratory scale in cross sections of microsamples of mortar layers^[4] and include hydrated compounds like gypsum ($\text{CaSO}_4 \cdot 2\text{H}_2\text{O}$), calcium oxalate compounds ($\text{CaC}_2\text{O}_4 \cdot 2\text{H}_2\text{O}$ and $\text{CaC}_2\text{O}_4 \cdot \text{H}_2\text{O}$), as well as mirabilite ($\text{Na}_2\text{SO}_4 \cdot 10\text{H}_2\text{O}$) and epsomite ($\text{MgSO}_4 \cdot 7\text{H}_2\text{O}$).

The extent of such degradations in the walls and wall paintings of two houses of Insula IX 3, mainly because of chemical attacks of atmospheric acid gases and biological colonization, was experimentally demonstrated through field spectroscopic analysis.^[10] Those field studies were performed under the Analytica Pompeiana Universitatis Vasconicae (APUV) project developed by the University of the Basque Country in cooperation with the Expeditio Pompeiana Universitatis Helsingiensis (EPUH) project of the Helsinki University^[11]; that work showed how the walls and wall paintings exposed to the rain-wash are the worst preserved.

This severe decay was not observed in the rooms covered by roofs; in these rooms, the most noticeable pathologies are the presence of high humidity in the walls and the high amount of efflorescence crystals. Nevertheless, if we compare photographic records from the past, one can appreciate another kind of damage that becomes severe with years. Figure 1 shows an example where the deterioration of the mural painting during the last 60 years is clearly seen; this painting is found in the north-west wall of the Triclinium (room 16) belonging to the House of Marcus Lucretius (house 5/24 in Insula IX 3), a room that has been covered by a roof for the last hundred years avoiding direct exposition to rain-wash events.

The explanation to the loss of details in the painted layer must be found in the continuous action of salt crystallization and dissolution processes. Salt crystallizations have been recently accounted as the single most important cause of deterioration of monuments in the Mediterranean Basin.^[12] Those phenomena are mostly related to acid dry deposition processes^[13] together with the presence of infiltration waters.^[14] In the particular case of the mural painting shown in Fig. 1, although being in a wall protected by roof, their back is exposed to rain; thus, fluxes of water at micrometric level are present inside the wall, favouring the movement of dissolved ions, the primary source for the formation of efflorescence crystals.

The study of efflorescence formation processes in the wall and wall painting remains of two houses in the Insula IX 3 of Pompeii

has been one of the objectives of the APUV project. Three different climatic conditions were acting on the houses during the field campaigns. Different orientations of the walls were taken into account in order to understand the salt formation process in the walls (with and without painted layers) as a function of the rain events, as well as the protection of the walls (covered and uncovered rooms by roofs) to the direct rain impact.

To perform the field analytical work, two portable spectroscopic instruments, Raman and energy dispersive X-ray fluorescence spectrometer (ED-XRF), were selected in order to have the molecular and the elemental information necessary to identify the compounds present in the efflorescence. Some years ago, we discussed the need for such a portable multi-analytical methodology to properly diagnose the conservation state of cultural heritage assets.^[15] Moreover, a systematic elemental concentration map on $1 \times 1 \text{ m}^2$ was constructed for the different walls, using the Kriging statistical procedure on the individual ED-XRF measurements performed over grids at about 10–20 cm.

To diagnose the causes of the efflorescence formation processes and to define the possible deterioration pathway(s), the chemical reactivity among original compounds and the acid gases was taken into account, following the procedures tested with very successful results in previous studies.^[4–6,13–15]

Experimental

Description of the studied houses and the climatic conditions

Two houses were thoroughly analyzed in the three measurement campaigns. The first house (House of Marcus Lucretius, IX 3, 5/24) has relatively well-preserved paintings, belonging to the fourth style of Roman wall paintings, with the majority of rooms covered by roof. The second analyzed house (the Dye House of Obonius, IX 3, 1-2) lies next to the House of Marcus Lucretius (refer to a plan of the House of Marcus Lucretius in Fig. 2) and is not as majestic in terms of decorative elements as the first one, but it has important remains of the first painting style. None of the rooms of the Dye House of Obonius is covered by roof. Details of both houses and their location within the Insula IX 3 are given elsewhere.^[4,11]

As already mentioned before, three areas were exhaustively monitored. The first case was the walls of rooms covered by roof, showing relatively well-preserved wall painting panels where red

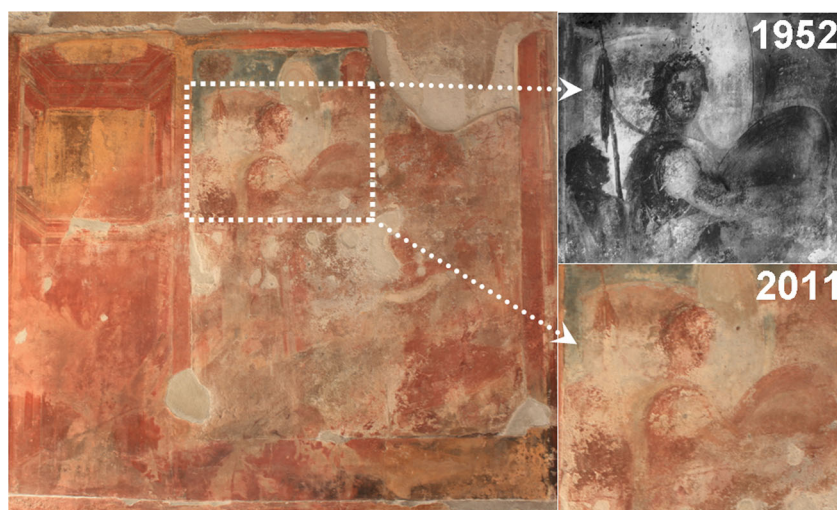


Figure 1. Detail of the decay observed over 60 years in the painted panel of the north-west wall of the triclinium (covered room 16, Marcus Lucretius House).

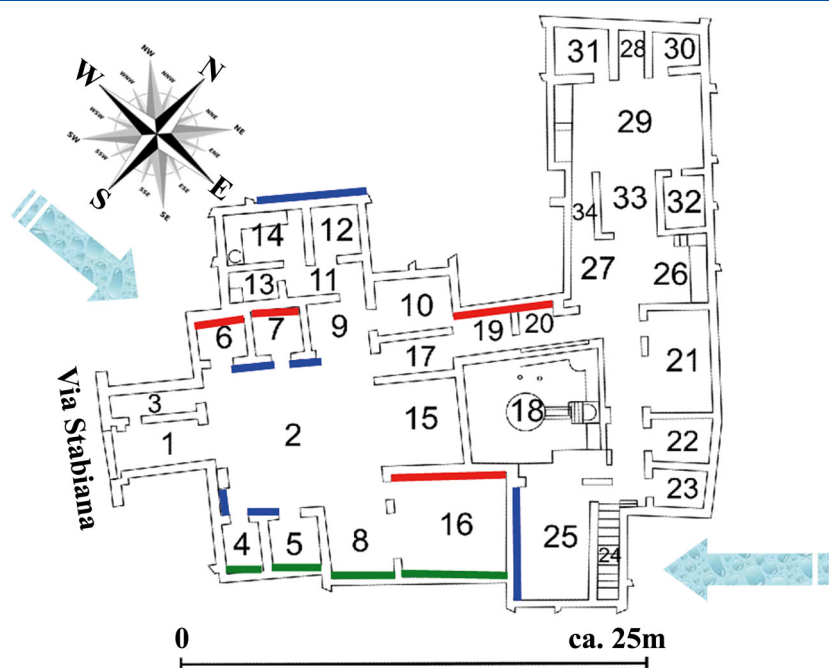


Figure 2. Plan of the Marcus Lucretius House showing the most intense winds, the two main directions of the rainfall and the three types of analyzed walls: (red line) covered walls having their back exposed directly to the rainfall, (green line) covered walls not affected by rainfall but affected by infiltration groundwaters and (blue line) non covered walls directly exposed to the rainfall. (This figure is available in colour online at wileyonlinelibrary.com/journal/jrs.)

ochre remains, mortars and efflorescence were analyzed in walls having their back directly exposed to rain events (refer to walls marked with red lines in Fig. 2). The second one was walls in covered rooms but not having their back oriented to the rain-wash (refer to walls marked with green lines in Fig. 2); thus, only infiltration waters from the ground can be considered as the wetting source of the walls. In these last walls, efflorescence crystals on yellow and red ochre panels were analyzed. Finally, the third area of the study was walls in rooms without roofs, totally exposed to rain, in which practically all the painting details have disappeared (refer to blue walls in Fig. 2), where the analyses were focused on the *intonaco* mortar layers and, when possible, the *arriccio* mortar layers.

Exposed and protected rooms were measured in spring (from the 10 to 16 of May 2010) and summer (from the 3 to 7 of September 2011 and from the 15 to 23 of September 2012). Spring 2010 had few rainfall events; therefore, a little amount of efflorescence was detected in the walls and practically nothing in the wall paintings of the protected rooms. The end of August 2011 was rainy, and the walls in the protected rooms, especially those oriented in their back to the main rainfall, were completely wet; some efflorescence crystals were 2 to 5 mm long. The beginning of September 2012 was also rainy; the walls were not wet when the measurements were performed, but in this case, a notable amount of efflorescence crystals, although less than in 2011, were evident even in the wall paintings of the covered rooms.

Hand-held spectrometers used to perform *in situ* measurements

The *in situ* analysis of the walls and wall paintings was carried out using hand-held instruments, as shown in Figure S1. In total, more than 250 spots were measured (sampled) during each analytical campaign, in order to guarantee representativeness of the acquired spectral information, i.e. on the chemical composition of the efflorescence crystals.

In order to obtain the mineralogical composition, Raman analysis was carried out with the portable inno-Ram spectrometer (B&W TEK INC., Newark, USA), equipped with a 785 nm excitation laser. The laser power is approximately 300 mW at the source and about 200 mW at the surface of the analyzed sample. The instrument implements a controller of the laser power fixable from 100 to 1% of the laser. The spectra range was acquired between 65 and 3000 cm^{-1} with a resolution of 4 cm^{-1} at 912 nm. The instrument implements a TE cooled (-20°C) back-thinned, 2D binning CCD detector. Raman spectra were recorded using the BWSpecTM 3.26 software version (B&W TEK INC.),^[10] after a daily calibration with a silicon chip using the 520.5 cm^{-1} Raman line. The interpretation of the unknown spectra was carried out by comparison with the collected Raman spectra of pure standard compounds inside the e-VISNICH dispersive Raman database.^[16] Additionally, free available Raman databases (e.g. UCL^[17] and RRUFF^[18]) were also considered for the assignment of the Raman bands.

The Raman microprobe was mounted on an X-Y-Z motorized tripod (DESINSO, Barcelona, Spain) that implements on its head a microcamera to focus onto the specific efflorescence crystals and also a webcam (Creative Live! Cam Optica AF) to acquire images of the whole area in which the spectrum is collected. The microprobe was mounted with an Olympus LMPlanFI 20 \times objective lens, having 12 mm working distance and 0.4 N.A. When the wind was causing excessive vibrations of the tripod at the moment of the measurement, the microprobe was handled manually.

In situ point-by-point elemental analysis was carried out using a hand-held ED-XRF from Innov-X Alpha Series[®] (Innov-X Systems Inc., Woburn, USA), which uses a miniature, low-power X-ray tube. The end-window is a transmission Ag-anode tube operating at up to 40 keV with a maximum current of 50 μA . A high-performance Si PiN thermo-electronically cooled diode detector with an energy resolution equal or less than 230 eV was used to detect and register the characteristic X-rays from the constituent elements of the analyzed materials. The system

was driven by a HP IPAQ pocket PC using Soil Mode software including identification of light elements (light element analysis program) up to phosphorous.

In order to obtain elemental distribution maps of the analyzed walls, another hand-held ED-XRF spectrometer, the XMET5100 (Oxford Instruments, UK), equipped with a calibration software based on fundamental parameters, was used. This analytical method allows obtaining semi-quantitative data even for the light elements, such as sulfur and sodium in our case. The equipment is provided with a rhodium X-ray tube as excitation source that works at a maximum of 45 keV (resolution of 0.2 keV at a maximum of 50 μ A of current) and includes a high-resolution silicon drift detector.

Statistical analysis and chemical reactivity simulations

To represent the concentration distribution of some compounds, a statistical analysis based on the Kriging procedure was performed. Geostatistics and spatial analysis have been widely used to quantify the spatial distribution of properties and concentration of elements and to identify possible 'hot spots'. To our knowledge, this procedure has not been applied until now over materials of the cultural heritage, although we have used it, for example, for environmental metal pollution monitoring in estuaries.^[19] Kriging refers to a group of spatial-statistical interpolation methods for assigning a value of a random field to points not physically analyzed based on the measured values in random fields at nearby locations in a data set. First, all concentrations in the mg/kg were changed into mmol/kg. The concentrations of the elements measured (as variable *x*) in a square each 10 or 15 cm (as variables *y* and *z*) by ED-XRF were used as data set to produce contour maps by Kriging interpolation using cross validation by means of the Surfer 8.0 software.

In order to define possible deterioration pathways, chemical reactivity simulations were performed through thermodynamic calculations using the MEDUSA^[20] software. Those simulations aim to explain the formation of new compounds (the so-called species in MEDUSA) as a consequence of chemical reactions among the original products (of walls and wall paintings) and the environmental compounds (atmospheric acid gases, ions dissolved in infiltration

waters, compounds from the metabolism of microorganisms, etc.), that are considered the components in MEDUSA. The construction of the thermodynamic (chemical) models, including the way to estimate the adequate values of the stoichiometric formation constants for the given equilibrium, is explained elsewhere.^[21] The *in situ* analyses will give us information about all the compounds; then, we must classify those compounds as originals (components of the chemical model) and new compounds (species formed after reactions among original and environmental compounds), following a methodology that has been applied in other studies of similar nature.^[4,5]

Results

The nature of the original mortars of the walls was earlier characterized by the use of Raman spectroscopy.^[4,5] The *arricio* layer is made with a typical calcite-sand mortar; calcite (CaCO_3) was identified as the original component of all the analyzed mortars, because of the systematic presence of bands at 1750 (w), 1607 (w), 1437 (m), 1086 (s), 712 (w) and 282 (m) cm^{-1} , as well as quartz (SiO_2), from the sand grains, detected by its main Raman band at 464 (s) cm^{-1} . The *intonaco* external layer showed also the presence of additional compounds such as calcium silicates and aluminates. They are typical of hydraulic lime mortars that used natural pozzolanic materials, being reported also the addition of natural calcitic fragments present in the Vesuvian ash.^[22] All these minerals, together with some metal carbonates derived from lime impurities like Na_2O and K_2O , must be considered as original compounds when searching for new products in the efflorescence crystals.

Table 1 summarizes all the compounds identified by *in situ* Raman analyses. As can be seen, calcite was determined as the original compound, detected usually by the bands reported in Table 1, being rather difficult to detect the minor bands when focusing in the efflorescence crystals. However, in these studies, natron ($\text{Na}_2\text{CO}_3 \cdot 10\text{H}_2\text{O}$) and potassium carbonate (K_2CO_3) were detected (not in the efflorescence but when analysing the *intonaco* layers), which should be considered as original compounds of the mortars.

The compounds shown in Table 1 have not been detected in all the campaigns, and their presence seems to be related to the climatic conditions and the exposure of walls to rainfall and/or infiltration groundwaters, as it is further discussed.

Table 1. Identified compounds by means of portable Raman spectroscopy on efflorescence and in the paint and *intonaco* layers

Mineral name	Molecular formula	Raman assignment (cm^{-1})	Effloresc.	<i>Intonaco</i> and paint layer	2010	2011	2012
Anhydrous nitrocalcite	$\text{Ca}(\text{NO}_3)_2$	1053m	X	X	X		
Niter	KNO_3	1048–1050w	X			X	X
Calcium monosulfoaluminate	$\text{Ca}_4\text{Al}_2\text{O}_6(\text{SO}_4)$	982w	X			X	X
Thenardite	Na_2SO_4	452m, 465m, 621m, 632m, 647m, 993s, 1101w, 1132w, 1152m	X		X	X	X
Mirabilite	$\text{Na}_2\text{SO}_4 \cdot 10\text{H}_2\text{O}$	447m, 616m, 626m, 989s, 1127w	X		X	X	X
Epsomite	$\text{MgSO}_4 \cdot 7\text{H}_2\text{O}$	984m	X		X	X	X
Bassanite	$\text{Ca}_2\text{SO}_4 \cdot \frac{1}{2}\text{H}_2\text{O}$	1014s	X				X
Gypsum	$\text{Ca}_2\text{SO}_4 \cdot 2\text{H}_2\text{O}$	1006–1008s, 1135w	X	X	X	X	X
Weddellite	$\text{CaC}_2\text{O}_4 \cdot 2\text{H}_2\text{O}$	188m, 505w, 910m, 1475s		X	X	X	X
Natron	$\text{Na}_2\text{CO}_3 \cdot 10\text{H}_2\text{O}$	1068m		X		X	
Potassium carbonate	K_2CO_3	1061m		X		X	
Calcite	CaCO_3	285m, 712w, 1086s		X	X	X	X
Hematite	$\alpha\text{-Fe}_2\text{O}_3$	225w, 293m, 409m, 494w, 610w		X	X	X	X

Efflorescence from walls having their back exposed to rainfall

The north(west) walls of five rooms (6, 7, 19, 20 and 16) covered by roofs were analyzed (refer to walls marked with red in Fig. 2). The mural painting shown in Fig. 1 belongs to the analyzed wall in room 16.

Almost all of the spectra collected on efflorescence in these rooms revealed the presence of one or several sulfate compounds, mostly in a lower hydrate form, i.e. bassanite instead of gypsum or thenardite instead of mirabilite (refer to Table 1 for chemical composition of the compounds). A typical Raman spectrum obtained in these walls is shown in Fig. 3, where the main band of bassanite ($\text{CaSO}_4 \cdot \frac{1}{2}\text{H}_2\text{O}$) and some bands of thenardite (Na_2SO_4) are seen. In particular, the areas directly exposed to the sunlight showed Raman spectra of nearly pure thenardite, as can be observed in Figure S2.

To elucidate if the concentration of the different compounds are uniformly distributed all along the walls, semi-quantitative ED-XRF element concentrations were measured in square grids and processed through the Kriging procedure. If the mg/kg concentration of sulfur is transformed into mmol/kg of calcium sulfate (gypsum), a map like the one shown in Fig. 3 is obtained. Two important conclusions can be drawn from that map: (a) the non-uniform distribution of the calcium sulfate concentration all along the wall and (b) the high value of the sulfate concentration, which is up to 4.6 mol/kg, that suggest a continuous impact (sulfation of calcite) without removing the new sulfate compounds as a result probably of the absence of a washing process in these covered rooms.

The same results were obtained in the other rooms when analysing the walls without pigment remains. A good example is the high concentration of sulfate compounds, suggesting an important impact on the original materials.

Efflorescence from walls not having their back exposed to rainfall

The south(east) walls of four rooms (4, 5, 8 and 16) covered by roofs were analyzed (refer to walls marked with green in Fig. 2)

within this category. Figure 4 shows two sets of Raman spectra obtained in the 2011 and 2012 campaigns on the same position of room 4. Two characteristic compounds in the unpainted areas of those rooms were identified, calcium monosulfoaluminate and thenardite, all over the calcite Raman signals. Their relative proportions changed from 1 year to the other, what suggests again the importance of the climatic conditions on the formation of the different compounds.

In addition, the walls in this category showed also an important efflorescence presence even in the painted areas, as can be observed in Fig. 5. Here, over the red hematite (room 8), Raman signals of gypsum (the most important sulfate compound on the painted areas), niter (KNO_3) and calcite were systematically recorded. In this case, the signal of calcite comes from the binder of the red-painted layer, so that should not be considered as an efflorescence or part of the mortar under the painted layer.

Figure 6 shows a nice view on the south(east) wall of room 8, where important white areas can be observed over the painted panels. It looks like these white areas have been formed as a consequence of an ascendant movement of the white salts. In that wall, a vertical profile of ED-XRF measurements was performed. Again, an average value of 0.9 mol/kg was obtained for calcium sulfate in the upper parts of the wall, while in the efflorescence, it shows a maximum value around 2.0 mol/kg, which is a really high concentration (refer to the bar graph in Fig. 6).

The Raman spectrum shown in Fig. 6 was collected on a poorly preserved mortar layer with pigment remains in the (south)west wall of room 8 (marked with the arrow). It shows the presence of niter together with hematite and calcite (pigment and binder respectively). This nitrate compound was also detected in the areas of south(east) wall of room 8 with painting remains, like that shown in Fig. 5.

The same trend is observed in the south(east) wall of room 16 (Figure S3). The ascendant profile of the white salts is clearly appreciated. In this case, the Raman analyses have showed, over the signals of calcite (again the binder of the painted

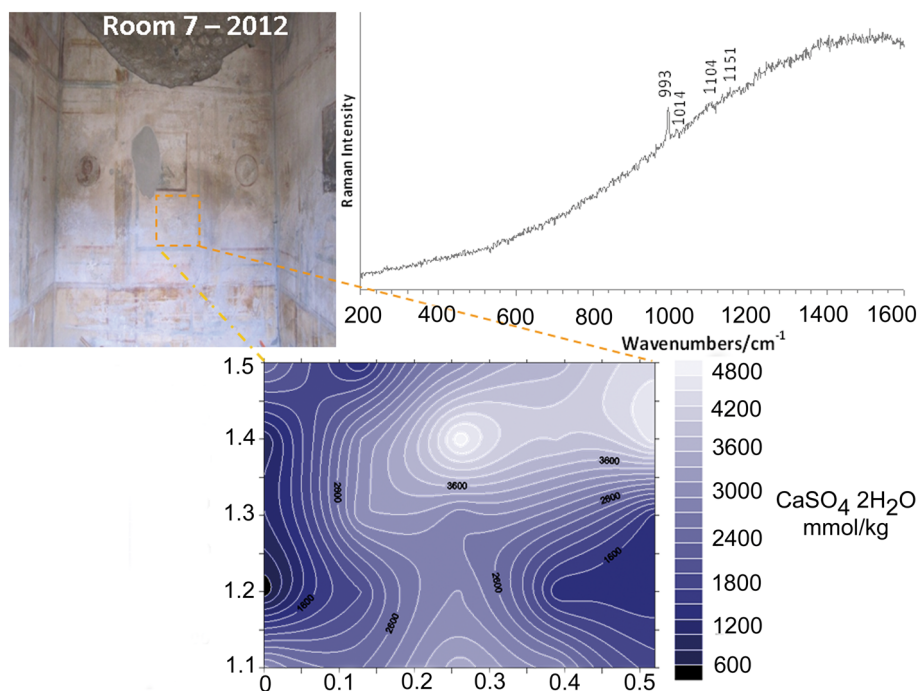


Figure 3. Raman spectrum taken on a efflorescence in the covered room 7 showing the presence of thenardite (Na_2SO_4) and bassanite ($\text{CaSO}_4 \cdot \frac{1}{2}\text{H}_2\text{O}$). Calcium sulfate distribution map (100 × 100 cm) with important fluctuations in the concentrations (<1.0–4.0 mol/kg).

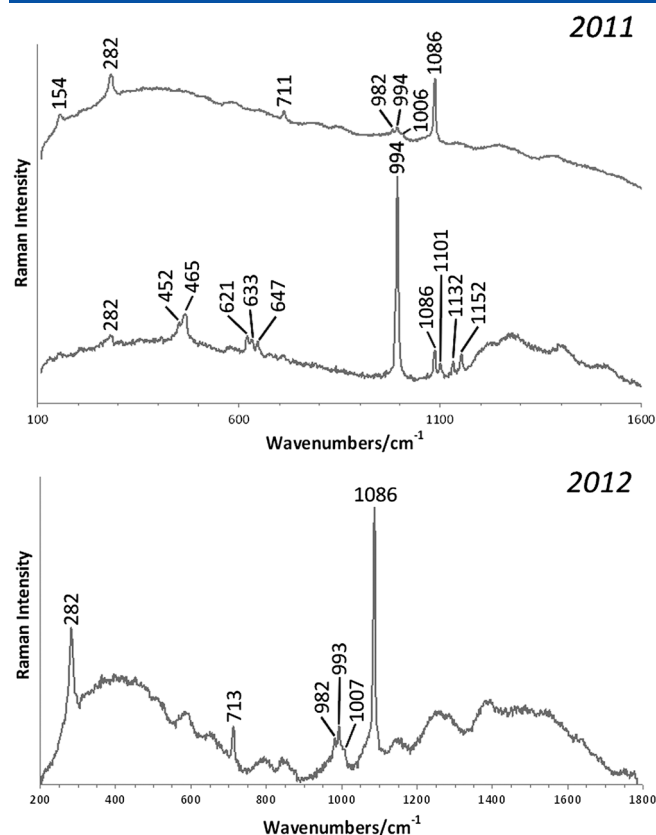


Figure 4. Raman spectra of some efflorescence compounds identified in the covered room 4. Apart from calcite, calcium monosulfoaluminate ($\text{Ca}_4\text{Al}_2\text{O}_6(\text{SO}_4)$, main Raman band at 982 cm^{-1}) and thenardite (Na_2SO_4) were identified in the 2011 campaign, whereas the 2012 campaign showed the same compounds but with inversed relative proportions.

layer), the presence of another sulfate compound, epsomite ($\text{MgSO}_4 \cdot 7\text{H}_2\text{O}$, main Raman band at 985 cm^{-1})^[4] together with niter (main Raman band at 1050 cm^{-1}).

In this case, the analyzed walls are not affected by the direct impact of the rainfall; thus, the influence of the infiltration waters from the ground must be taken into account. In these rooms (refer to the green walls in Fig. 2), the dropping rain from the roofs, discharging directly in the back of the walls, is probably the source of the water incoming to the materials through capillarity. Moreover, this water is again the vehicle to dissolve partially some of the compounds, moving their free ions and precipitating the same (or other) compounds when the wall is dried. This is clearly observed in the contour map of gypsum presented in Figure S4, which belongs to the south(east) wall of room 5. In this plot, variable concentrations are observed, from less than 0.6 mol/kg to nearly 2.0 mol/kg . These concentrations are half of the ones observed in the walls having their back affected by direct rainfall (refer to Fig. 3).

Efflorescence from walls exposed directly to rainfall

The walls of four rooms (2, 12, 14 and 25), not covered by roofs, were analyzed (refer to walls marked with blue lines in Fig. 2). These walls have lost all the details of the painted layers, having only small – near microscopic – remains of pigment grains. The damage is so important that even the intonaco layer has been lost in some of the areas and thus revealing the arriccio layer.

The CO_2 attack on non-protected walls is the greatest decaying event accompanied by rain wash of the highly soluble metal

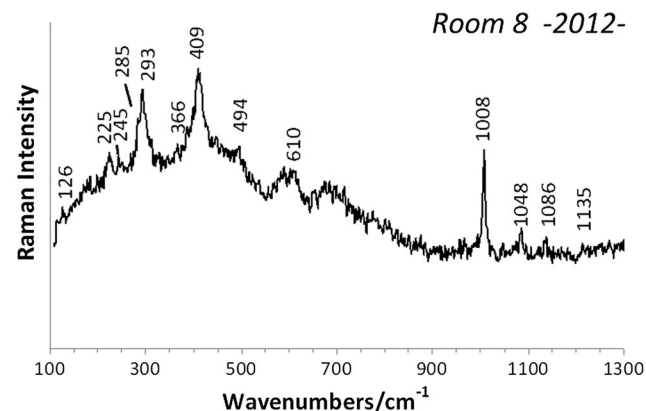


Figure 5. Image of perfectly formed efflorescence crystals over the red ochre polychromy in the covered room 8. The Raman spectrum shows, over the signals of hematite, a complex mixture with gypsum ($\text{CaSO}_4 \cdot 2\text{H}_2\text{O}$) as the main compound and niter (KNO_3) and calcite (CaCO_3) as the other white substances.

bicarbonate salts formed after the acid attack (decarbonation of wall paintings and plaster layers until observation of the arriccio mortar).^[10] However, bicarbonate salts were not found *in situ*, and only calcium, sodium and potassium carbonate (CaCO_3 , Na_2CO_3 , K_2CO_3) were identified by Raman spectroscopy. All of them can be considered original compounds in the mortars as explained before. In particular, the potassium source must be attributed to the manufacturing of the original mortar when the local groundwaters of the potassium bicarbonate type were used^[23] and/or quick lime with an important K_2O presence (around 1%)^[24] was used. This is consistent with the nearly constant potassium background concentration, measured by ED-XRF in all the areas where the intonaco and/or arriccio layers were accessible to the direct analysis.

Gypsum was again the main compound detected in such washed walls, probably because it is a partially soluble compound (only 1800 mg/kg are dissolved leaving free Ca^{2+} and SO_4^{2-} ions) and most of it remains as a solid phase. Figure 7 shows two Raman spectra measured in the wall of room 25, one belongs to mirabilite ($\text{Na}_2\text{SO}_4 \cdot 10\text{H}_2\text{O}$) and the other to weddellite ($\text{CaC}_2\text{O}_4 \cdot 2\text{H}_2\text{O}$). These two highly hydrated compounds have only been measured in walls directly exposed to rain-wash, i.e. walls with a high level of humidity all over the year.

Moreover, the presence of weddellite must be considered as a bio-signature of some microorganisms that colonized the walls with a permanent exposure to the rainfall, as demonstrated in previous works.^[4,10,24] In this case, the presence of oxalate is attributed to the metabolic activity (excretion of oxalic acid) of microorganisms and not to the degradation of organic binders/waxes, because

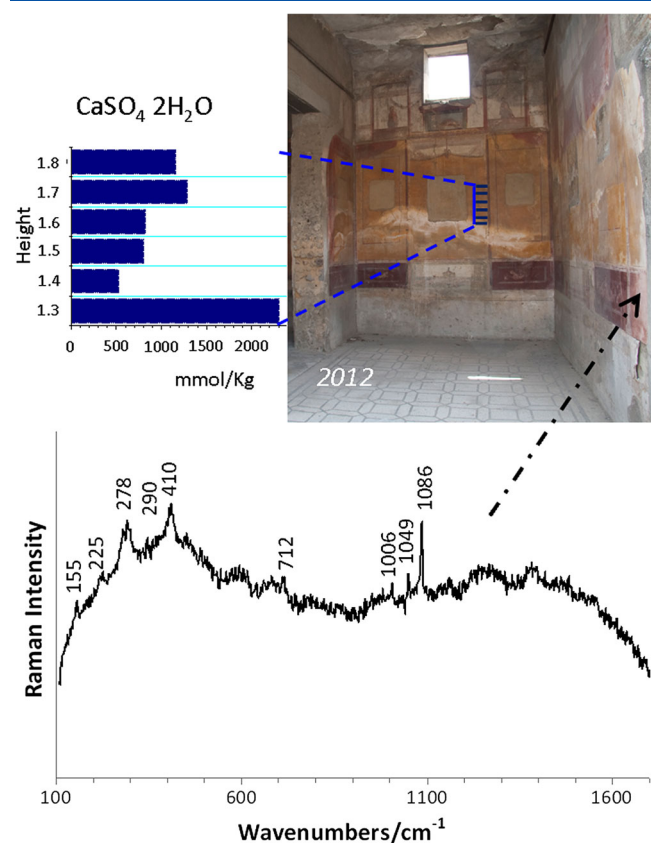


Figure 6. Vertical gypsum profile on the south wall (their back is not exposed to direct rainfall) of the covered room 8, showing the important concentration on the whitest part of the wall. The Raman spectrum shows small bands of hematite (α -Fe₂O₃), the presence of calcite (CaCO₃) and niter (KNO₃), together with traces of gypsum (CaSO₄·2H₂O).

other excreted compounds (such as some carotenoids) were simultaneously present.^[10,25]

To elucidate the influence of the orientation of the walls in the uncovered rooms, three walls of room 2 were analyzed in 2011 by ED-XRF and Kriging to obtain the contour maps of gypsum shown in Fig. 8. In this sense, the north and west walls of room 2 appeared to have the lowest gypsum concentrations, while the relatively most protected wall has more gypsum concentrations. Irrespective of the concentration values, the distribution of gypsum is not uniform. Moreover, this distribution changes within the year, as can be observed in Figure S5 where the maps of 2011 and 2012 for the north wall of room 2 are plotted.

Finally, the comparison of gypsum concentrations as a function of the type of room must be highlighted. The lowest concentrations are recorded for the ones directly exposed to rain-wash, whereas the highest concentrated ones are those in the walls of protected rooms but with the rainfall effect on their back. This experimental observation suggests that apart from the damage caused by the direct rain-wash events, the negative influence of the infiltration waters from the ground can be considered also an important source of damage, even for those walls belonging to rooms covered by roof.

Chemical simulations and decaying pathways

The conversion of the original calcium carbonate (binder and mortar layers) in the different nitrate and sulfate forms cannot be explained by the direct action of water dissolution. The dissolved

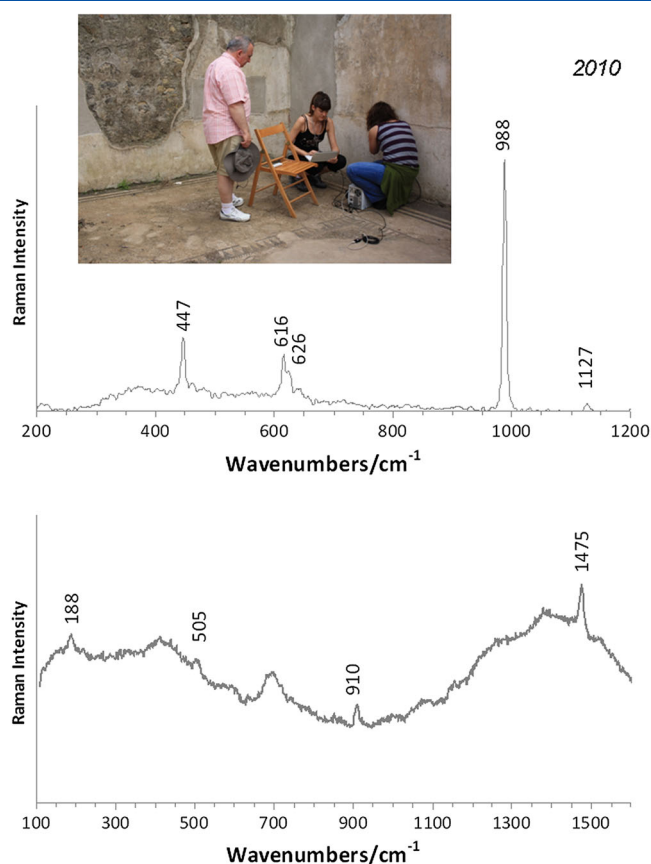


Figure 7. Raman spectra on efflorescence crystals of the most exposed wall of the non-covered room 25 to rainfall. They showed systematically the presence of mirabilite (Na₂SO₄·10H₂O) and weddellite (CaC₂O₄·2H₂O).

amount of calcium carbonate in water is negligible, and the Ca²⁺ concentration released is extremely low to reach the saturation condition of the identified calcium nitrate and calcium sulfate compounds. The chemical reactivity simulations performed with the MEDUSA software have showed the need of an acid to neutralize the carbonate anion.

The required acids are present in the modern atmosphere around Pompeii, having not only CO₂ but also SO₃ and N₂O₅ when the anthropic sulfur oxide and nitrogen oxide compounds are oxidized by the ozone.^[26]

The reaction of calcium carbonate with carbonic acid is irreversible, producing soluble Ca²⁺ and HCO₃⁻ ions, which can be washed out from the walls during a rainfall episode in the exposed rooms.

The reaction of calcium carbonate with sulfuric acid produces calcium sulfate and CO₂ gas that disappears to the atmosphere. The chemical reactivity of calcite against atmospheric SO₂ has been explained elsewhere.^[4]

The reaction of calcium carbonate with nitric acid is also irreversible producing calcium nitrate and CO₂ gas. As the calcium nitrate is more soluble than the calcium sulfate forms, this compound must be detected after a pronounced period without rainfall episodes, like the one during our 2010 analytical campaign. This compound was not detected in the 2011 and 2012 campaigns that were more wet (refer to Table 1), and consequently, the calcium nitrate was probably washed out from the walls after its formation.

The reactivity of potassium carbonate against nitric acid is like that of calcium carbonate. However, potassium nitrate is so soluble that is deliquescent. Thus, its presence in exposed walls is hard to

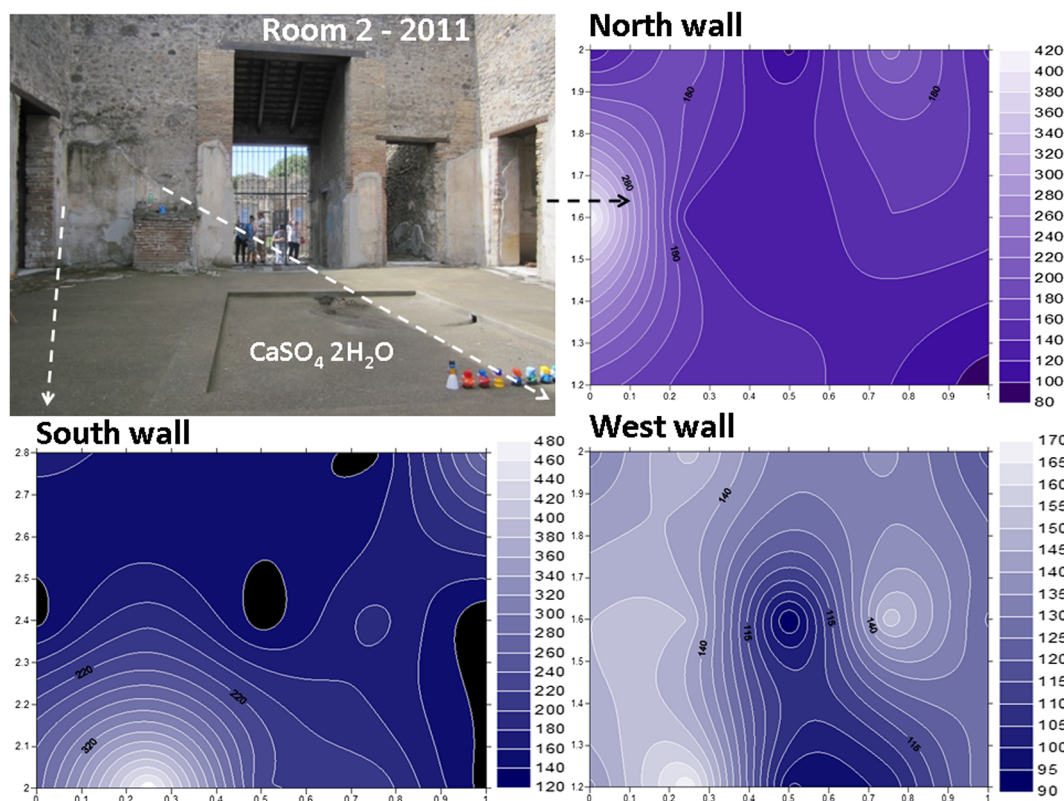
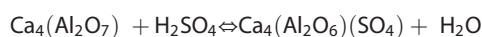


Figure 8. Contour maps of gypsum ($\text{CaSO}_4 \cdot 2\text{H}_2\text{O}$) in three walls (north, west and east) of the non-covered atrium (room 2), showing a non-constant distribution of the calcium sulfate concentrations, as well as different concentration levels depending on the orientation of each wall to the rainfall.

be detected but, in covered rooms, niter is not dissolved and is systematically detected in such rooms. Details of the chemical reaction leading to the formation of nitrate salts are given elsewhere.^[13,14]

Finally, the presence of calcium monosulfoaluminate must be highlighted. Its presence in the original hydraulic mortars must be discarded because it is formed in the presence of gypsum, a compound that was not present in the original mortars. However, as the concentration of gypsum has increased with years (especially in the covered rooms as a result of the absence of washing process), as well as that of sulfuric acid aerosol, calcium monosulfoaluminate can be formed by reaction of tetra calcium aluminate (one compound present in the hydraulic mortars) with sulfuric acid:



or alternatively with dissolved sulfate ions and free protons that can be present in highly degraded areas with absence of basic carbonates.

Conclusions

The APUV expeditions (2010, 2011 and 2012) were focused on the analyses of walls and wall paintings from two houses of Insula IX, 3 (houses 1,2 and 5,24); some rooms of greater importance are covered with ceilings, but most of them are exposed to open air. During the analytical campaigns, the nature of the efflorescence covering the walls and wall paintings was evaluated using portable, non-destructive spectroscopic instrumentation. Raman spectroscopy was used to obtain the molecular composition and energy dispersive X-ray fluorescence for the elemental analysis.

These field works confirmed a systematic presence of decaying compounds in the efflorescence crystals growing on the mortars and even on the painted layers of the walls, such as sulfates (mainly gypsum but also calcium monosulfoaluminate, thenardite, mirabilite and epsomite) and nitrates (anhydrous nitrocalcite and niter).

Modelling of chemical reactions and statistical Kriging procedures were used to explain the results of quantitative concentrations. This has resulted in a model that explains the deterioration process in terms of chemical reactivity, taking into account the orientations of the walls as well as the covered and not covered rooms analyzed in Insula IX 3.

In non-protected rooms, formed sulfate and nitrate salts can be dissolved by water reaching the surface or inside the walls, and this is one of the reasons for the disappearance of the wall painting panels exposed at rain-wash. A low-cost protecting action to slow down the loss of materials could be the covering of rooms with ceilings. The authorities should take into account that the acid attack, coming from natural or anthropogenic sources, is always waiting to new disposable calcite, and other carbonates, to form soluble compounds that will be the cause for the formation of new efflorescences.

In covered rooms, the nature and concentration of sulfate and nitrate salts vary with time, climate conditions and orientation of the walls. In protected wall paintings and walls, higher sulfur contents were observed (severe sulfation decay) in comparison to the lower amount of sulfur in exposed walls. Sulfates with higher water content were observed in protected rooms where the wall was wet, i.e. those having their back in front of the main wind (and rain falls) direction.

The extended presence of nitrate salts in the efflorescence is clearly because of NO_x attack, being less probable as a consequence of the impact of infiltration waters (the expected NH_4NO_3 load must be low because of the absence of organic materials

around the walls at ground level). Nonetheless, the source of potassium (niter has been systematically found in all covered rooms) must be further investigated because the ED-XRF measurements gave variations of one order of magnitude between the lower and higher potassium concentration values.

Acknowledgements

The authors would like to thank the Soprintendenza Speciale per i Beni Archeologici di Napoli e Pompeii, for the permissions to perform our field studies during the 2010, 2011 and 2012 expeditions, as well as the Finnish EPUH project group, especially Emeritus Professor Paavo Castren and Docent Antero Tammisto from Helsinki University, for the support given to our spectroscopic measurements in the houses of the Insula IX, 3. A. Giakoumaki and A. Pitarch are grateful to the University of the Basque Country (UPV-EHU) for their post-doctoral contracts. The English revision by Dr. Gorka Arana is gratefully acknowledged.

This work was financially supported by the projects DEMBUMIES (ref. BIA2011-28148), funded by the Spanish Ministry of Economy and Competitiveness (MINECO), and Global Change and Heritage (ref. UFI11-26), funded by the University of the Basque Country (UPV-EHU). The accompanying actions CTQ2010-10810-E (MINECO), AE11-27 (UPV-EHU) and AE12-32 (UPV-EHU) supported the expeditions APUV2010, APUV2011 and APUV2012 respectively.

References

- [1] A. Varone, Pompeii. I misteri di una città sepolta-Storia e segreti di un luogo in cui la vita si è fermata duemila anni fa. Newton Compton Editori, Roma (2005).
- [2] K. Keune, J. J. Boon, *Anal. Chem.* **2005**, *77*, 4742.
- [3] M. Cotte, J. Susini, N. Metrich, A. Moscato, C. Gratzu, A. Bertagnini, M. Pagano, *Anal. Chem.* **2006**, *78*, 7484.
- [4] M. Maguregui, U. Knuutinen, K. Castro, J. M. Madariaga, *J. Raman Spectrosc.* **2010**, *41*, 1400.
- [5] M. Maguregui, U. Knuutinen, I. Martinez-Arkarazo, K. Castro, J. M. Madariaga, *Anal. Chem.* **2011**, *83*, 3319.
- [6] M. Maguregui, K. Castro, H. Morillas, J. Trebolazabala, U. Knuutinen, R. Wiesinger, M. Schreiner, J. M. Madariaga, *Anal. Methods* **2014**, *6*, 372.
- [7] I. Aliatis, D. Bersani, E. Campani, A. Casoli, P. P. Lottici, S. Mantovan, I-G Marino, *J. Raman Spectrosc.* **2010**, *41*, 1247.
- [8] M. Castriota, V. Cosco, T. Barone, G. de Santo, P. Carafa, E. Cazzanelli, *J. Raman Spectrosc.* **2008**, *39*, 295.
- [9] P. Baraldi, C. Baraldi, R. Curina, L. Tassi, P. Zannini, *Vibr. Spectrosc.* **2007**, *43*, 420.
- [10] M. Maguregui, U. Knuutinen, I. Martinez-Arkarazo, A. Giakoumaki, K. Castro, J. M. Madariaga, *J. Raman Spectrosc.* **2012**, *43*, 1747.
- [11] Expeditio Pompeiana Universitatis Helsingiensis, The Pompeii Project of the University of Helsinki, <http://blogs.helsinki.fi/pompeii-project/> (last accessed on 2014 July 11th).
- [12] R. M. Espinosa-Marzal, G. W. Scherrer, *Account Chem. Res.* **2010**, *43*, 897.
- [13] A. Sarmiento, M. Maguregui, I. Martinez-Arkarazo, M. Angulo, K. Castro, M. A. Olazabal, L. A. Fernandez, M. D. Rodriguez-Laso, A. M. Mujika, J. Gomez, J. M. Madariaga, *J. Raman Spectrosc.* **2008**, *39*, 1042.
- [14] M. Maguregui, A. Sarmiento, I. Martinez-Arkarazo, M. Angulo, K. Castro, G. Arana, N. Etchebarria, J. M. Madariaga, *Anal. Bioanal. Chem.* **2008**, *391*, 1361.
- [15] K. Castro, S. Pessanha, N. Proietti, E. Princi, D. Capitani, M. L. Carvalho, J. M. Madariaga, *Anal. Bioanal. Chem.* **2008**, *391*, 433.
- [16] M. Maguregui, N. Prieto-Taboada, J. Trebolazabala, N. Goienaga, N. Arrieta, J. Aramendia, L. Gomez-Nubla, A. Sarmiento, M. Olivares, J. A. Carrero, I. Martinez-Arkarazo, K. Castro, G. Arana, M. A. Olazabal, L. A. Fernandez, J. M. Madariaga, ChemCH, 1st Internacional Congress on Chemistry for Cultural Heritage, Rabean, 30th June-3rd July, **2010**.
- [17] L. Burgio, R. J. H. Clark, *Spectrochim. Acta A* **2001**, *57*, 1491.
- [18] R. T. Downs, Program and Abstracts of the 19th General Meeting of the International Mineralogical Association, Kobe, Japan. **2006**, <http://rruff.info> (last accessed on 2014 July 11th).
- [19] S. Fdez-Ortiz de Vallejuelo, A. Gredilla, A. de Diego, G. Arana, J. M. Madariaga, *Sci. Tot. Environ.* **2014**, *473*, 473–474, 359.
- [20] I. Puigdomenech, A. Zagorodni, M. Wang, M. Muhummed, *Program Medusa (Make Equilibrium Diagrams Using Sophisticated Algorithms)*. Royal Institute of Technology, Inorganic and Materials Chemistry, Sweden, **2007**.
- [21] J. C. Raposo, J. Sanz, G. Borge, M. A. Olazabal, J. M. Madariaga, *Fluid Phase Equilibria*. **1999**, *155*, 1.
- [22] D. Miriello, D. Barca, A. Bloise, A. Ciarallo, G. M. Crisci, T. De Rose, C. Gattuso, F. Gazineo, M. F. La Russa, *J. Archaeol. Sci.* **2010**, *37*, 2207.
- [23] S. Caliro, G. Chiodini, R. Avino, C. Cardellini, F. Frondini, *Appl. Geochem.* **2005**, *20*, 1060.
- [24] Mineralogy and Chemistry of Raw Materials & Products, St Astier Natural Hydraulic Limes (NHL). <http://www.stastier.co.uk/nhl/testres/minchem.htm> (last accessed on 2014 July 11th).
- [25] M. Maguregui, U. Knuutinen, J. Trebolazabala, H. Morillas, K. Castro, I. Martinez-Arkarazo, J. M. Madariaga, *Anal. Bioanal. Chem.* **2011**, *402*, 1529.
- [26] A. Boselli, M. Armenante, L. D'Avino, M. D'Isidoro, G. Pisani, N. Spinelli, X. Wang, *Boundary-Layer Meteorol.* **2009**, *132*, 151.

Supporting information

Additional supporting information may be found in the online version of this article at the publisher's web site.